Published in J. Phys. D: Appl. Phys. vol. 40 , 2162-2169 (2007)

A non-standard shear resonator for the matrix characterization of piezoceramics and its validation study by finite element analysis

L Pardo[1], M Algueró[1] and K. Brebøl[2]
[1]Instituto de Ciencia de Materiales de Madrid (ICMM). Consejo Superior de Investigaciones Científicas (CSIC). Cantoblanco 28049- Madrid (Spain).
[2]Limiel ApS. Langebæk (Denmark).

E-mail: lpardo@icmm.csic.es, malguero@icmm.csic.es, kbreboel@post3.tele.dk

Abstract. Standard shear samples used for piezoceramic characterization lead to underestimation of the piezoelectric shear coefficients due to its dynamical clamping at resonance. This work presents the application of Alemany et al.´s automatic iterative method to the resonance of a non-Standard shear sample, in order to determine the related complex parameters of piezoceramics, thus including losses, from impedance measurements. The matrix of dielectric, elastic and piezoelectric complex parameters that fully characterize a piezoceramic, a 6mm symmetry material, can be obtained from such shear data combined with the application of the method to three other electromechanical resonances, namely: the length extensional mode of long rods or rectangular bars, length poled; the thickness extensional mode of a thin plate or disk, thickness poled, and the radial mode of a thin disk, thickness poled. Shear results are here obtained for non-Standard samples of a commercial Navy type II piezoceramic, solving the underestimation of the coefficients in the Standard shear sample and allowing the improvement of the previously reported characteristic matrix from Standard samples. Three-dimensional Finite Element Analysis (FEA) modelling of the resonances of the three material samples used in the matrix characterization was here accomplished using the improved matrix of dielectric elastic and piezoelectric material coefficients including all losses. The comparison of the experimental resonance spectra of this piezoceramic samples and the FEA results obtained for the elastically, dielectrically and piezoelectrically homogeneous items modelled is here presented and discussed.

PACS numbers: 77.65.-j; 77.84.Dy ; 02.70.Dh; 06.20 fb; 43.20 Ks.

1. Introduction

The modelling and design of piezoelectric devices by, among others, Finite Element Analysis (FEA) methods, rely on the accuracy of the dielectric, piezoelectric and elastic coefficients of the active material used, commonly an anisotropic poled ferro-piezoelectric ceramic [1], a piezoceramic.

Poled ferro-piezoelectric ceramics in their normal low voltage operating range show substantially linear relations between the stress (T_{ij}) and the strain (S_{ij}), which are tensor magnitudes, on the one hand, and between the electric field (E_i) and the dielectric displacement (D_i), which are vector magnitudes, on the other. Besides, the piezoelectric coefficients provide relations between the mechanical and the electrical magnitudes. Piezoceramics, which have 6mm symmetry, are characterized by only five independent elastic constants, three independent piezoelectric coefficients and two independent dielectric coefficients. The constitutive equations can take various forms [1] and, thus, there are various sets of parameters, related among them, that characterize a piezoceramic. Here we choose to work with the following coefficients: s_{11}^E ,

s_{12}^E, s_{13}^E, s_{33}^E, s_{44}^E and s_{66}^E (note that $s_{66}^E = 2\,(s_{11}^E - s_{12}^E)$); d_{13}, d_{33} and d_{15}; ε^S_{11} and ε^S_{33}, , as they are those requested by the FEA software used.

The accurate description of piezoceramics involves the evaluation of the dielectric, piezoelectric and mechanical losses, taking into account the out of phase material response to the external excitation, which is not always accomplished, despite of the important role of the losses in the material performance. Losses in piezoceramics are a problem for positioning actuator applications, for they cause hysteresis in the field-induced strain, and for resonance applications, such as ultrasonic transducers, piezoelectric transformers and motors, for they cause heat generation. On the other hand, they can be an advantage for force sensors and acoustic transducers, because they widen the frequency band for receiving signals. The origin of the losses in ferroelectric ceramics has been analyzed in numerous works [2-5]. While the dielectric losses are related to the ionic and the ferroelectric nature of these compounds, the mechanical losses in piezoceramics arise from crystal lattice defects, microstructure (grain boundaries, porosity) and ferroelastic domain wall motions [6] and the piezoelectric losses for the coupling of all such effects. The description of the material parameters by complex values [7] ($P^* = P' - iP''$) is a convenient way to separately account for the dielectric, piezoelectric and mechanical losses ($\tan\delta = P''/P'$).

Characterization methods for poled ferro-piezoelectric ceramics from impedance measurements at the electromechanical resonances, providing their dielectric, piezoelectric and elastic coefficients in the linear range, have been used since early times of the development of these materials in the 60´s. The first Standard measurement procedures of piezoceramics [8] have been revised and updated several times, the most recent ones being issued by the North American institutions “American National Standards Institute (ANSI)” and “The Institute of Electrical and Electronic Engineers (IEEE)” in 1987 [9]. However, the 1987 IEEE Standard does not account for the complex nature of the material coefficients. Nevertheless, 1987 IEEE Standard contribution to the characterization of piezoelectric ceramics is, of course, remarkable. The 1987 IEEE Standard states the resonator shapes, their boundary conditions for the validity of the equations used and all the relationships among the coefficients needed to get all the independent coefficients for piezoceramics. European Standards kept these shapes and ratios among sample dimensions [10].

Several authors [11-14] developed methods for the complex characterization of piezoceramics from complex impedance (or its reciprocal, the complex admittance) measurements at resonance, which validity has been analyzed elsewhere [15,16]. Alemany et al. developed an automatic iterative method, applied in a first publication [17] to four modes of resonance used in the Standards: (1) the length extensional mode of a thickness poled rectangular bar; (2) the length extensional mode of long rods or rectangular bars, length poled; (3) the thickness extensional mode of a thin plate or disk, thickness poled, and (4) the thickness shear mode of an in-plane poled thin plate. In a second publication the method was also applied to (5) the radial mode of a thin disk, thickness poled [18], the most mathematically complex geometry to be solved.

Four modes of resonance of the three sample shapes shown in figure 1(a), (b) and (c), namely the mentioned 2, 3, 4 and 5 modes, are sufficient [19] for the purpose of the determination of the full set of

complex coefficients of piezoceramics in the matrix of a 6mm symmetry material. These modes are listed in Table 1, which also shows the directly obtained coefficients for each mode. The systematic application of the automatic iterative method to the matrix characterization, including losses, of a Navy type II, soft lead zirconate titanate (PZT) commercial piezoceramic (PZ27 of Ferroperm Piezoceramics A/S (Kvistgård, Denmark)), using the three Standard samples shapes and four resonance modes of Table 1, has been already accomplished [19]. However, the shear piezoelectric coefficient d_{15} reported for PZ27 [19] is underestimated (d_{15}=396pC.N^{-1}) by the measurement of the Standard shear resonator, with respect to the actual value quoted by the manufacturer [20] (d_{15} = 500pC.N^{-1}), which is obtained from direct measurements on accelerometers working with shear elements. A similar underestimation was obtained [21] for Motorola 3203HD piezoceramic, for which resonance of such Standard shear geometry gave an electromechanical coupling coefficient of k_{15}=61%, whereas the manufacturer states k_{15}=72% as catalogue value [22].

This matrix of complex coefficients [19] allows the modelling by FEA of PZ27 piezoceramic items of a given geometry. Three-dimensional FEA modelling of the three Standard material resonators used in the above mentioned matrix characterization has recently been carried out [23, 24]. These FEA results reproduce, in the dielectrically, elastically and piezoelectrically homogeneous Standard shear item that was modelled, and provide an explanation of the secondary resonances in the vicinity of the fundamental shear resonance. Such spurious resonances were generally, and erroneously according to the FEA results, associated to microstructural or poling inhomogeneities of the piezoceramic. The dynamical clamping of the Standard shear sample, that was previously suggested by other authors [25], is revealed by FEA modelling [23] and has also been verified by laser interferometry measurements [26]. This finding also helped to explain why the use of the Standard shear geometry led to underestimation of the shear piezoelectric coefficients. Because of this underestimation, some discrepancies between experimental and FEA modelled resonance spectrum were also revealed for the thickness resonance of a thin disk, that does not follows a piston-like motion but involves relevant shear stresses [24]. An improvement of the matrix characterization already reported for a Navy type II piezoceramic, which involves the results from the Standard shear sample, has been proved as a need for the purpose of FEA modelling of samples of this piezoceramic. This improvement involves a more accurate determination of the shear piezoelectric coefficients.

This work presents the application of Alemany et al.´s automatic iterative method to the resonance of a non-Standard shear geometry in order to obtain, from impedance measurements, the related piezoceramic parameters. The shear results obtained from this geometry for a commercial piezoceramic, PZ27 of Ferroperm Piezoceramics A/S, are used to get an improved set of characteristic dielectric, elastic and piezoelectric complex coefficients of this material. Three-dimensional FEA modelling of the new set of samples used in this characterization was accomplished using the improved matrix of material coefficients. The comparison of the experimental resonance spectra of these samples and the FEA results obtained for elastically, dielectrically and piezoelectrically homogeneous modelled samples, based on this improved

characteristic matrix, is presented here to validate the material data obtained from measurements on the non-Standard geometry.

2. Experimental procedure

2.1. Automatic iterative method applied to a non-Standard shear mode

The non-Standard shear sample shape here considered (figure 1(d)) is that of the second thickness shear resonance mode, already described by Berlincourt [27], and that was later analyzed by other authors [25, 28, 29]. The following formula [25] is used as the the analytical solution of the wave equation for the second thickness shear resonance mode of motion, when the dimensional ratio given by t >> w (figure 1(d)) is fulfilled:

$$Y = G + iB = i\frac{2\pi f w L \varepsilon_{11}^{s}}{t} + i\frac{2we_{15}^{2}}{t}\sqrt{\frac{s_{55}^{E}}{\rho}}\tan\left(\pi f L\sqrt{\rho s_{55}^{E}}\right) \qquad (1)$$

In the method here used for the above described shear sample, the coefficients e_{15}, ε^{S}_{11} and s^{E}_{55} (note that $s^{E}_{55} = s^{E}_{44} = 1/c^{E}_{55}$) are calculated by solving - using an automatic iterative numerical method as previously described [17] - of the set of non-linear equations that results when experimental complex admittance data are introduced into this analytical expression. Such admittance data are needed at four frequencies in the neighborhood of the resonance and antiresonance peaks, being the determination of such frequencies also automatic in this method.

In principle, only the value of the complex admittance or impedance at such four frequencies around the resonance, together with the dimensions and density of the sample, are required to get the coefficients e_{15}, ε^{S}_{11} and s^{E}_{55}. The same can be said for all other resonance modes here considered, except for the radial mode of thin disks, for which it is additionally needed to know the value of $f^{(2)}_{s}$, the frequency for maximum conductance, G, of the first overtone [18]. In practice, an experimental data file of absolute values of admittance, $|Y|_i$, and its phase angle, θ_i, at each frequency, f_i, is obtained in a frequency interval around the resonance. From these values, the corresponding values of conductance, $G_i = |Y|_i \cos\theta_i$, and resistance $R_i = \cos\theta_i\, |Y|_i^{-1}$ are obtained. Two of the four frequencies involved in the calculation, f_s and f_p, are determined by location of the maximum values of R_i and G_i in the measured interval, and the values of complex impedance at such frequencies introduced in the system of non-linear equations to be solved, in the so-called central iteration of the method. The determination of the other two frequencies involved in the calculation of the central iteration, f_1 and f_2, constitutes a second iterative process, called peripherial iteration of the method [17], which finish when the convergence of f_2 fulfils the criteria:

$$|f_2(\text{final}) - f_2(\text{initial})| < 0.05\%.$$

Contrary to what it is done in the fitting methods, both the G and the R profiles are reconstructed here just as a quality criteria of the results obtained by the method, since the solution of the equation system

is unique and cannot be further modified. Such reconstruction is done by insertion of the obtained complex coefficients in the analytical solution of the wave equation of the given resonance mode and calculation of R and G as a function of frequency. When the experimental resonance spectrum is free of spurious resonances, thus corresponding to a single resonator, the agreement factor between the experimental and reconstructed values is usually above 0.99, which underlies the quality of the method.

2.2. Finite Element Analysis

The FEA modelling was done using ATILA software [30]. Originally developed for modelling sonar transducers, this program has the ability to include piezoelectric materials defined by a full data set of complex variables. The three dimensional harmonic analysis, here used, yields the impedance values in a given interval of frequencies, from which the resonance and antirresonance frequencies and the electromechanical coupling factors can be obtained.

The three sample shapes modelled (figure 1(a), (c) and (d)) here were those of the samples used to determine the improved set of dielectric, elastic and piezoelectric complex coefficients, namely: (1) a thin ceramic disk [19] of diameter D=37,80 mm and thickness t=0,76 mm, thickness poled, (2) a long bar, lenght poled [19], of D=2mm and length L= 20mm and (3) thickness poled non-Standard shear plates here suggested (figure 1(d)) with actual dimensions W=0.9mm, t=8.97mm and L=8.1mm. The mesh used in each resonator simulation was selected so as to have a minimum of five nodes per wavelength, except the shear elements which were divided into a 30x30x3 mesh consisting of 2700 hexagonal 20 node elements. This very fine mesh was used to include the secondary resonances found in the experimental spectrum which has a wavelength much smaller than the one of the main resonance. The number of frequencies analyzed was chosen so as to get a compromise between the time of the simulation and the required resolution of the calculated spectrum, depending of its complexity. The disk and the long bar were simulated as rotationally symmetric items, which results in calculation times of the order of a few minutes for the whole frequency sweep in a PC with a Pentium IV, 3GHz, processor. The shear elements were simulated as full three-dimensional items, resulting in 15 minutes calculation time for each discrete frequency point.

3. Experimental results and discussion

3.1. Shear resonance mode of the non-Standard shear geometry

Figure 2(a) shows the experimental spectrum and the reconstructed G and R peaks of a non-Standard shear sample, using Formula 1 and the coefficients obtained after its solution by Alemany et al.´s method. The reproduction of the main resonance (frequency and height of the R and G peaks) is highly accurate. This shear sample does not present a unique resonance for the dimensional ratios here considered, t≈10W, but the main resonance is clearly more intense than the secondary ones and thus is appropriated for the material characterization. Table 2 shows the comparison between all the parameters obtained from an

Standard shear sample and one of those here studied. These parameters are the ones directly obtained by this method and also those that can be calculated from them using known relations [19]. The losses are lower from all the elastic coefficients determined from the non-Standard shear geometry and the real part of dielectric permittivity is higher, whereas the dielectric losses are also slightly lower. The non-Standard shear geometry yielded, as seeked, a real part of the piezoelectric coefficient of d_{15}=526 $pC.N^{-1}$, closer to the actual value in devices [20].

The matrix of complex coefficients of the piezoceramic (figure 3) was obtained taking into account the average values of the coefficients obtained from the four non-Standard shear samples measured and considering an average of the two values of ε^{T}_{33} measured [19], obtained from the length resonance of the long bar and from the planar resonance of the thin disk, in the calculation of all derived parameters. The Holland [2] criteria for the piezoceramic to be passive, in the sense of not being an energy generator, was verified for the values of the matrix in figure 3.

Figure 2(b) shows the experimental and FEA modelled resonance spectrum of a non-Standard shear sample. The resonance and antiresonance frequencies are quoted in Table 3, showing good agreement (differences below 2%) with the experimental ones. The height of the FEA modelled G peaks is also in good agreement, whereas the R peak modelled is slightly lower. One has to note also to understand this that the experimental dispersion in R values of the peaks in the measured samples is also higher than the dispersion in the G peaks.

Secondary resonance peaks near the shear plate resonance are reproduced also by the FEA analysis, corresponding to an elastically, dielectrically and piezoelectrically homogeneous piezoceramic item, and the modelled frequencies are in good agreement with the measured ones (Table 3). Thus, these resonances being due to inhomogeneities (due to poling, composition of microstructure) of the material can also be disregarded for this shear geometry.

One of the problems to obtain a consistent set of data from different samples is that it is difficult to get the same level of polarization in all of them. Depending on the ceramic crystal anisotropy, and more markedly when poling at saturation conditions is not achieved, it has been found, by measurements of thermocurrent induced by propagation of low frequency thermal waves through the ceramic, that the polarization level is lower at an skin, of a given thickness depending on the poling conditions, of the samples [31, 32]. The in-plane poled Standard shear sample has a higher surface/volume ratio for poling than the thin disk, thickness poled, and polarization homogeneity level in both samples is expected to be different. The new shear sample reduces this problem since the thin disk and shear plate, both thickness poled, under the same poling conditions are expected to have the same polarization and polarization homogeneity level.

3.2. Length extensional resonance mode of a long bar

Figure 4 shows the experimental and FEA modelled resonance spectrum of a long bar. The resonance and antiresonance frequencies and electromechanical coupling factors are quoted in Table 3, showing good agreement (differences below 1%). The height of the R and G peaks modelled by FEA is also in reasonable agreement with the experimental values. This good agreement is however obtained independently of the shear coefficients used [24], since this mode of vibration is purely dilatational.

3.3. Radial resonance mode of a thin ceramic disk

Figure 5 shows the experimental and FEA modelled resonance spectrum of the radial mode of the thin disk. Again, the resonance and antiresonance frequencies and electromechanical coupling factors are also quoted in Table 3, showing once more good agreement with experimental values (differences below 1%), which also takes place for the height of the R and G peaks. The planar mode is also independent of shear coefficients, since it is also purely dilatational [24].

3.4. Thickness extensional resonance mode of a thin ceramic disk

Figure 6(a) shows the experimental and FEA modelled resonance spectrum of the thickness mode of a thin disk, using the matrix of coefficients obtained from the Standard shear sample [24]. There is a clear discrepancy in the comparison of the experimental and modelled resonance and antiresonance frequencies. As already mentioned [24] the mode of motion of the thickness mode involves a non-negligible shear stress and thus is sensitive to the accuracy of the shear coefficients used. figure 6(b) shows the same experimental and FEA modelled resonance spectrum of the thin disk, now modelled using the matrix of figure 3. Frequencies and electromechanical coupling factors are quoted in Table 3 also for this resonance mode. For the FEA modelling with this improved matrix of material coefficients, we found that differences in the modelled frequencies with respect to the experimental that are below 1%. The height of the R and G peaks modelled by FEA shows also a reasonable agreement, validating the results of the measurement from the non-Standard shear sample.

4. Conclusions

This work presents the application of Alemany et al.´s automatic iterative method to the resonance of a non-Standard thickness poled shear geometry, in order to determine the related complex material coefficients, from complex inmittance measurements, and the results for a Navy II type commercial piezoceramic. The value of the real part of the piezoelectric shear coefficient d_{15} obtained is higher than the one previously reported from measurements of Standard shear samples, dynamically clamped, and agrees with that derived from measurement of actual shear samples in devices.

The spectra of the four resonance modes of the three sample shapes, including the non-Standard shear sample, needed for the matrix characterization of the studied piezoceramic have been modelled by FEA. The improved matrix of complex material coefficients, including shear coefficients from the non-

Standard sample, was used in the modelling. A good reproduction of both the experimental peaks of conductance, G, and resistance, R, at resonance was achieved by the FEA modelling for all modes studied.

FEA results reproduce, in addition to those R and G peaks of the main resonance, those of the secondary modes in the elastically, dielectrically and piezoelectrically homogeneous shear item modelled. Sample inhomogeneities are thus disregarded as the origin of such secondary resonances.

The radial resonance of the thin disk and the length extensional resonance of a long bar corresponds to purely dilatational vibration modes, given the dimensional ratios stablished for the standard samples, and the agreement between the frequencies for the FEA modelling and the experimental ones is within 2%. Finally, the influence of correctly determined shear coefficients on the also accurate reproduction of the frequency of the thickness mode of resonance of a thin disk is also revealed by FEA results, which previously showed that relevant shear contributions to the mode of motion at thickness resonance occurs.

Overall, the FEA study validates the improved matrix of parameters obtained using the non-Standard shear geometry here studied, the second thickness shear geometry described by Berlincourt, which provides a more homogeneous set of samples for the matrix characterization of piezoceramics.

Acknowledgements

This work was carried out under Spanish projects MAT 2001-4819-E, MAT2004-00868, and has benefited from the sinergy provided by the POlar ELEtroCERamics, POLECER, (G5RT-CT2001-05024) Thematic Network of the EC. Authors are indebted to W.W.Wolny and E. Ringaard from Ferroperm Piezoceramics A/S (Kvistgård, Denmark) for the ceramic samples used in this study. C. Alemany and A. García (holder of a POLECER-CAM co-funded FINNOVA grant at ICMM-CSIC) are acknowledged for some of the measurements carried out for this work. Authors are also especially indebted to C. Alemany (ICMM-CSIC, at the time of writing this paper already retired) for the generous implementation of the automatic iterative method to the second thickness shear geometry here used and thoughtfull discussions of the work.

References

[1] Jaffe B, Cook WR and Jaffe H. Piezoelectric Ceramics. Academic Press. London, 1971. pp.8-10.

[2] Haerdtl KH 1982 Electrical and mechanical losses in ferroelectric ceramics" *Ceram Int.* **8** 121.

[3] Uchino K and Hirose S 2001 Loss mechanisms in piezoelectrics: How to measure different losses separately" *IEEE Trans. on Ultrasonics, Ferroelectrics and Frequency Control* **48** 307.

[4] Robert G, Damjanovic D and Setter N 2001 Piezoelectric hysteresis analysis and loss separation. *J. Appl. Phys.* **90**(9) 4668.

[5] Mezheritsky AV 2004 Elastic, Dielectric and Piezoelectric Losses in Piezoceramics: How It Works All Together *IEEE Trans. on Ultrasonics, Ferroelectrics and Frequency Control* **51**(6) 695.

[6] Moulson AJ and Herbert JM Electroceramics. Materials, Properties and Applications. Chapman and Hall. London, 1990. pp. 69-76.

[7] Holland R 1967. Representation of dielectric, elastic and piezoelectric losses by complex coefficients. *IEEE Trans.Sonics Ultrason.* **SU-14**(1) 18.

[8] IRE standard on piezoelectric crystals: Measurements of piezoelectric ceramics, 1961, *Proc. IRE*, **49**(7) 1161-1169 (1961).

[9] IEEE Standard on piezoelectricity. *ANSI/IEEE Std.* 176-1987.

[10] Piezoelectric properties of ceramic materials and components. Part 2: methods of measurement – Low power *European Standard CENELEC*, EN 50324-2.

[11] Smits JG. 1976 Iterative method for accurate determination of the real and imaginary parts of the materials coefficients of piezoelectric ceramics. *IEEE Trans. Sonics Ultrason.* **SU-23**(6) 393.

[12] Sherrit S., Wiederick HD and Mukherjee BK 1992 Non-iterative Evaluation of the Real and Imaginary Material Constants of Piezoelectric Resonators. *Ferroelectrics* **134** 111.

[13] Tsurumi T, Kil YB, Nagatoh K, Kakemoto H and Wada S 2002 Intrinsic Elastic, Dielectric, and Piezoelectric Losses in Lead Zirconate Titanate Ceramics Determined by an Immittance-Fitting Method *J.Am.Ceram.Soc.* **85**(8) 1993.

[14] Hong Du X, Wang QM and Uchino K 2003 Accurate Determination of Complex Materials Coefficients of Piezoelectric Resonators *IEEE Trans. on Ultrasonics, Ferroelectrics and Frequency Control* **50**(3) 312.

[15] Kwok KW, Chan HLW and Choy CL 1997 Evaluation of the Material Parameters of Piezoelectric Materials by various methods *IEEE Trans. on Ultrasonics, Ferroelectrics and Frequency Control* **44**(4) 733.

[16] Pardo L, Alemany C, Ricote J, Moure A, Poyato R and Agueró M. Iterative methods for characterization of piezoelectric materials with losses. *Proc. of Internacional Conference on Technology and Design of Integrated Piezoelectric Devices, A POLECER Symp.*, 2-4 February, 2004. Courmayeur (Italy).

[17] Alemany C, Pardo L, Jiménez B, Carmona F,Mendiola J and González AM 1994 Automatic iterative evaluation of complex material constants in piezoelectric ceramics *J. Phys. D: Appl. Phys.* **27** 148.
[18] Alemany C, González AM, Pardo L, Jiménez B, Carmona Fand Mendiola J 1995 Automatic determination of complex constants of piezoelectric lossy materials in the radial mode *J. Phys. D: Appl.Phys.* **28**(5) 945.
[19] Algueró M, Alemany C, Pardo L and Gonzalez AM 2004 Method for obtaining the full set of linear electric, mechanical and electromechanical coefficients and all related losses of a piezoelectric ceramic *J. Am. Ceram. Soc.* **87**(2) 209.
[20] http://www.ferroperm-piezo.com
[21] Sherrit S, Wiederick HD and Mukherjee BK 1997 A complete characterization of the piezoelectric, dielectric and elastic properties of Motorola PZT3203HD including losses and dispersion *Medical Imaging 1997: Ultrasonic Transducer Engineering, SPIE Proc.***3037** 158.
[22] http://www.ctscorp.com/components/Datasheets/PZT.pdf
[23] Pardo L, Algueró M and Brebøl K 2005 Resonance modes in Standard piezoceramic shear geometry: A discussion based on Finite Element Analysis *J. Physique IV France* **128** 207.
[24] Pardo L, Algueró M and Brebøl K Resonance modes in Standard Characterization of Piezoceramics: A discussion based on Finite Element Analysis *Ferroelectrics* **336** 181.
[25] Aurelle N, Roche D, Richard C and Gonnard P Sample aspect ratio influence on the shear coefficients measurements of a piezoelectric bar *Proc. 9th IEEE Iternacional Symposium on Applications of Ferroelectrics (ISAF)*. Eds. R.K. Pandey, M. Liu and A. Safari. The Pennsylvania State University, University Park, PA, USA. August 7-August 10, 1994. pp. 162-165.
[26] Pardo L, Montero de Espinosa F and Brebøl K 2006 Study by laser interferometry of the resonance modes of the shear plate used in the Standards characterization of piezoceramics *Journal of Electroceramics* (in press).
[27] Berlincourt DA, Curran DR and Jaffe H Piezoelectric and Piezomagnetic Materials and Their Function in Transducers in Physical Acoustics vol.1. Part A. Ed. W.P. Mason, Academic Press, 1964. p.230.
[28] Cao W, Zhu S and Jiang B 1998 Analysis of the shear modes in a piezoelectric vibrator *Journal of Applied Physics* **83** 4415.
[29] Comyn T, Tavernor AW 2001 Aspect ratio dependence of d_{15} measurements in Motorola 33203 material *Journal of the European Ceramic Society* **21** 12.
[30] ATILA User´s Manual, Institut Superieur d´Electronique du Nord, Acoustics Laboratory (1997).
[31] de Frutos J and Jiménez B 1990 Study of the spatial distribution of the polarization in ferroelectric ceramics by means of low frequency sinusoidal thermal waves *Ferroelectrics* **109** 101.
[32] de Frutos J and Jiménez B 1992 Evolution of the spatial distribution of polarization in lead-calcium ferroelectric ceramics *Ferroelectrics* **126** 341.

Figure Captions

Figure 1. (a), (b) and (c): samples shapes and dimension ratios used in the Standard piezoelectric characterization and (d) non-Standard shear geometry used in this work. P=sample polarization.

Figure 2. (a) Experimental data and reconstructed resistance, R, and conductance, G, from the obtained shear parameters and for the fundamental shear thickness resonance of a non-Standard shear geometry of the Navy II type commercial PZT. (b) The same experimental data and the FEA modelled resistance, R, and conductance, G, using the improved matrix of parameters of Figure 3.

Figure 3. The improved matrix of parameters. Data are given in the following units: s^E_{ij} (10^{-12} m^2N^{-1}), d_{ij}(10^{-12} CN^{-1}) and ε_o = 8,859 x 10^{-12} Fm^{-1}

Figure 4. Experimental data and FEA modelled resistance, R, and conductance, G, using the improved matrix of parameters and for the fundamental length extensional resonance of a long bar, length poled, of the Navy II type commercial PZT.

Figure 5. Experimental data and FEA modelled resistance, R, and conductance, G, using the improved matrix of parameters and for the fundamental radial resonance of a thin disk, thickness poled, of the Navy II type commercial PZT.

Figure 6. Experimental data and FEA generated resistance, R, and conductance, G, for the fundamental thickness resonance of a thin disk, thickness poled, of the Navy II type commercial PZT, (a) using the matrix of parameters including those obtained from the IEEE Standard shear geometry (ref.19) and (b) using the improved matrix of parameters of Figure 3.

Table Captions

Table 1. The three Standard sample shapes and four modes of resonance needed for the matrix characterization of ferro-piezoelectric ceramics with 6mm symmetry.

Table 2. Coefficients obtained for shear resonance modes of the Standard and the non-Standard samples used here. Marked in bold those coefficients directly obtained by solving the equation of movement in the non-Standard shear mode.

Table 3. Experimental values of resonance and antiresonance peaks and their Q values (ratio between maximum frequency and width at half-maximum) and electromechanical coupling factors, obtained by Alemany et al.´s method, k_{ij}, and effective, $k_{eff} = (1- (f_s/f_p)^2)^{1/2}$, and FEA generated values of the same, for the four resonance modes studied, including the non-Standard shear geometry for the Navy II type commercial PZT ceramic.

Table 1. The three Standard sample shapes and four modes of resonance needed for the full characterization of ferro-piezoelectric ceramics with 6mm symmetry.

Sample geometry	Resonance mode	Directly obtained coefficients
• thin disks, thickness poled	• thickness extensional mode of thin plates	• h_{33}, ε^S_{33}, c^D_{33}
	• radial mode of thin disks	• d_{31}, ε^T_{33}, s^E_{11}, s^E_{12}
• shear plates	• thickness shear mode of thin plates	• h_{15}, ε^S_{11}, c^D_{55}
• long bars, length poled	• length extensional mode of long bars	• g_{33}, ε^T_{33} , s^D_{33}

Table 2. Coefficients obtained for shear resonance modes of the standard and the non-standard samples used here of a Navy II type commercial PZT. Marked in bold those coefficients directly obtained by solving the equation of movement in the non-Standard shear mode.

SHEAR MODE	In-plane poled STANDARD Shear sample[19]	Thickness poled NON-STANDARD Shear sample
k_{15} (%)	61.86	67.02
N_{15} (kHz.mm)	925	829
c_{55}^D (10^{10} N.m^{-2})	3.99 + 0.09i	3.84 + 0.06i
c_{55}^E (10^{10} N.m^{-2})	2.44 + 0.11i	2.11 + 0.06i
s_{55}^D (10^{-12} m^2.N^{-1})	25.25 - 0.54i	26.06 – 0.43i
s_{55}^E (10^{-12} m^2.N^{-1})	40.85 + 1.82i	**47.30 – 1.29i**
h_{15} (10^8 V.cm^{-1})	15.54 + 0.16i	15.56 +0.24i
e_{15} (C.m^{-2})	9.74 - 0.26i	**11.07- 0.14i**
d_{15}(10^{-12} C.N^{-1})	397.51 – 28.22i	523.54 – 20.73i
g_{15} (10^{-3} mVN^{-1})	39.25 + 0.44i	40.57 + 0.05i
$\varepsilon_{11}^T(\varepsilon_0)$	1144.40 – 68.47i	1457.63 – 55.85i
$\varepsilon_{11}^S(\varepsilon_0)$	707.79 – 25.94i	**803.28 – 21.93i**

Table 3. Experimental values of resonance and antiresonance peaks and their Q values (ratio between frequency at the maximum and width at half-maximum) and electromechanical coupling factors, obtained by Alemany et al.´s method, k_{ij}, and effective, $k_{eff} = (1- (f_s/f_p)^2)^{1/2}$, and FEA generated values of the same, for the four resonance modes studied, including the non-Standard shear geometry for the Navy II type commercial PZT ceramic.

	k(%)	Q_S	Q_P	f_s(kHz)	G_{max}(Siemens)	f_p(kHz)	R_{max}(Ohms)
Second Thickness Shear resonance of a thin plate							
experimental	$\|k_{15}\| = 67.02$ $k_{eff} = 60.0$	69	69	921	8.85×10^{-4}	1151	3.34×10^{5}
FEA	$k_{eff} = 61.0$	28	35	929	8.18×10^{-4}	1172	1.68×10^{5}
Lenght extensional resonance of long bar							
experimental	$\|k_{33}\| = 67.22$ $k_{eff} = 63.4$	71	131	71.0	3.56×10^{-5}	91.8	4.99×10^{7}
FEA	$k_{eff} = 64.4$	60	105	70.6	2.97×10^{-5}	92.3	6.21×10^{7}
Radial resonance of thin disk							
experimental	$\|k_P\| = 58.18$ $k_{eff} = 51.2$	98	160	53.5	0.190	62.3	6268.1
FEA	$k_{eff} = 52.3$	99	153	53.6	0.192	62.9	6147.7
Thickness resonance of thin disk							
experimental	$\|k_t\| = 48.24$ $k_{eff} = 44.4$	102	94	2494	4.44	2784	121.6
FEA	$k_{eff} = 43.3$	83	138	2492	4.81	2764	104.0

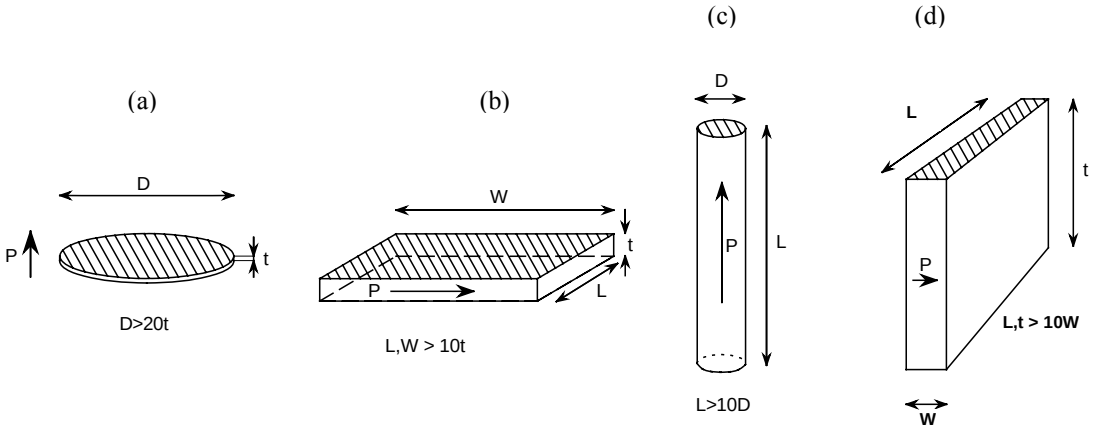

Figure 1. (a), (b) and (c): samples shapes and dimension ratios used in the Standard piezoelectric characterization and (d) non-Standard shear geometry used in this work. P=sample polarization.

(a)

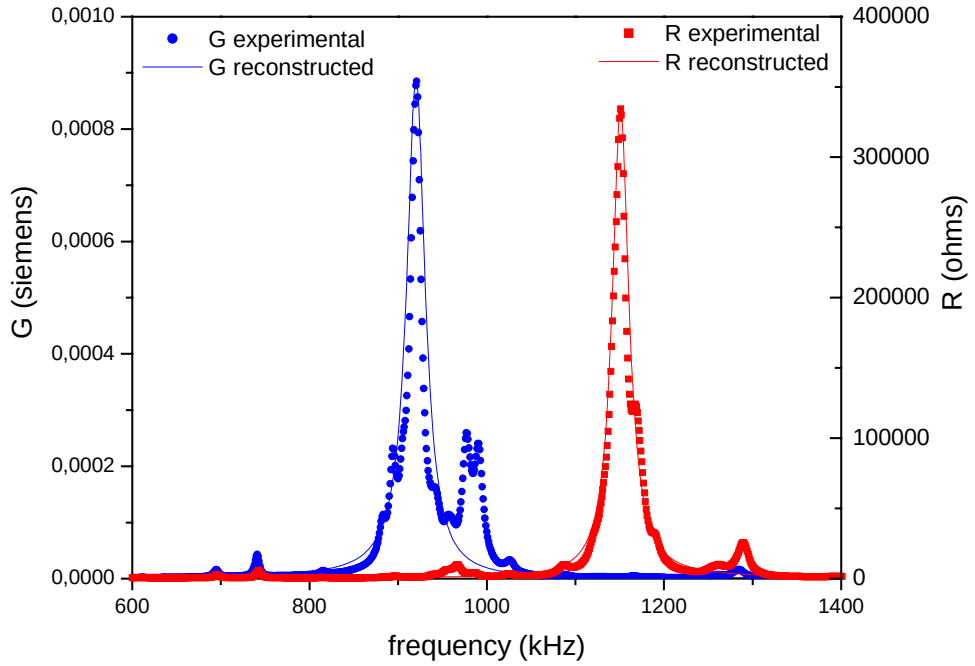

(b)

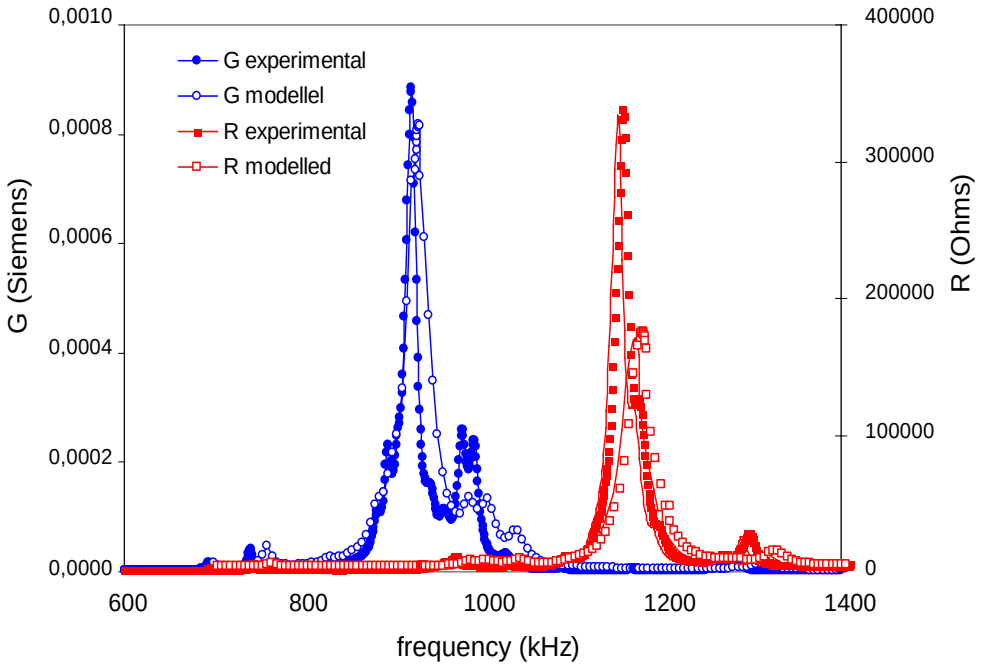

Figure 2. (a) Experimental data and reconstructed resistance, R, and conductance, G, from the obtained shear parameters and for the fundamental shear thickness resonance of a non-Standard shear geometry of a Navy II type commercial PZT. (b) The same experimental data and the FEA modelled resistance, R, and conductance, G, using the improved matrix of parameters of Figure 3.

$$\left(\begin{array}{cccccc|ccc} s_{11}^E & s_{12}^E & s_{13}^E & 0 & 0 & 0 & 0 & 0 & d_{31} \\ s_{12}^E & s_{11}^E & s_{13}^E & 0 & 0 & 0 & 0 & 0 & d_{31} \\ s_{13}^E & s_{13}^E & s_{33}^E & 0 & 0 & 0 & 0 & 0 & d_{33} \\ 0 & 0 & 0 & s_{44}^E & 0 & 0 & 0 & d_{15} & 0 \\ 0 & 0 & 0 & 0 & s_{44}^E & 0 & d_{15} & 0 & 0 \\ 0 & 0 & 0 & 0 & 0 & s_{66}^E & 0 & 0 & 0 \\ \hline 0 & 0 & 0 & 0 & d_{15} & 0 & \varepsilon_{11}^S & 0 & 0 \\ 0 & 0 & 0 & d_{15} & 0 & 0 & 0 & \varepsilon_{11}^S & 0 \\ d_{31} & d_{31} & d_{33} & 0 & 0 & 0 & 0 & 0 & \varepsilon_{33}^S \end{array}\right) = \left(\begin{array}{ccccccccc} 16{,}1-0{,}17i & -5{,}9+0{,}06i & -6{,}5+0{,}11i & 0 & 0 & 0 & 0 & 0 & -160+3{,}1i \\ -5{,}9+0{,}06i & 16{,}1-0{,}17i & -6{,}5+0{,}11i & 0 & 0 & 0 & 0 & 0 & -160+3{,}1i \\ -6{,}5+0{,}11i & -6{,}5+0{,}11i & 17{,}7-0{,}26i & 0 & 0 & 0 & 0 & 0 & 344-6{,}8i \\ 0 & 0 & 0 & 47{,}17-1{,}3i & 0 & 0 & 0 & 526-18{,}0i & 0 \\ 0 & 0 & 0 & 0 & 47{,}17-1{,}3i & 0 & 526-18{,}0i & 0 & 0 \\ 0 & 0 & 0 & 0 & 0 & 44{,}0-0{,}46i & 0 & 0 & 0 \\ 0 & 0 & 0 & 0 & 526-18{,}0i & 0 & (784-22{,}3i)\varepsilon_0 & 0 & 0 \\ 0 & 0 & 0 & 526-18{,}0i & 0 & 0 & 0 & (784-22{,}3i)\varepsilon_0 & 0 \\ -160+3{,}1i & -160+3{,}1i & 344-6{,}8i & 0 & 0 & 0 & 0 & 0 & (822-10{,}3i)\varepsilon_0 \end{array}\right)$$

Figure 3. The improved matrix of parameters of a Navy II type commercial PZT. Data are given in the following units: s^E_{ij} (10^{-12} m^2N^{-1}), d_{ij} (10^{-12} CN^{-1}) and ε_o = 8,859 x 10^{-12} Fm^{-1}

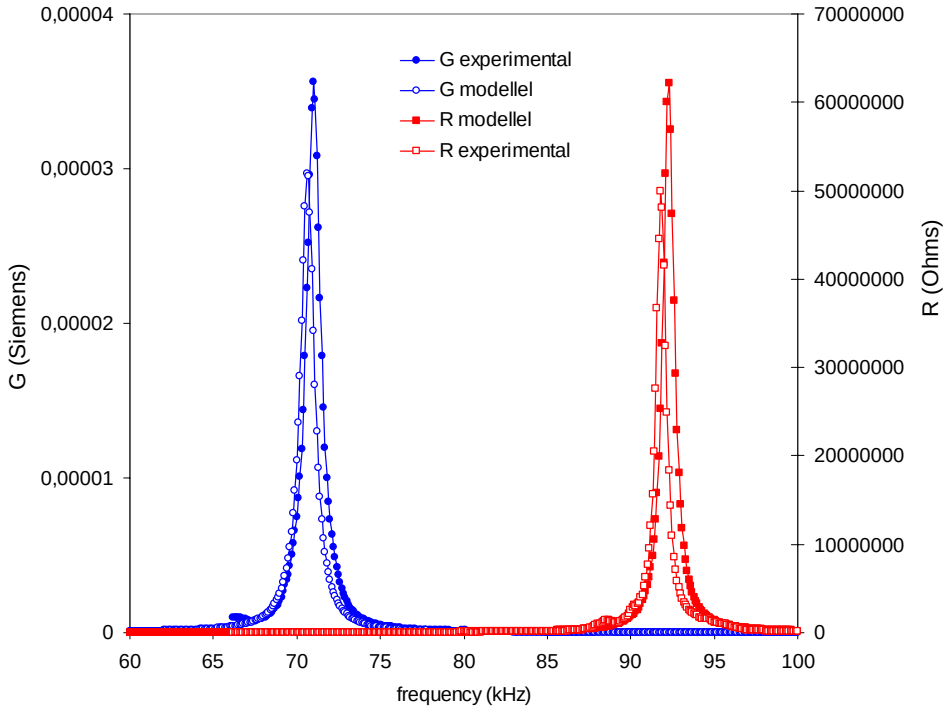

Figure 4. Experimental data and FEA modelled resistance, R, and conductance, G, using the improved matrix of parameters and for the fundamental length extensional resonance of a long bar, lenght poled, of a Navy II type commercial PZT.

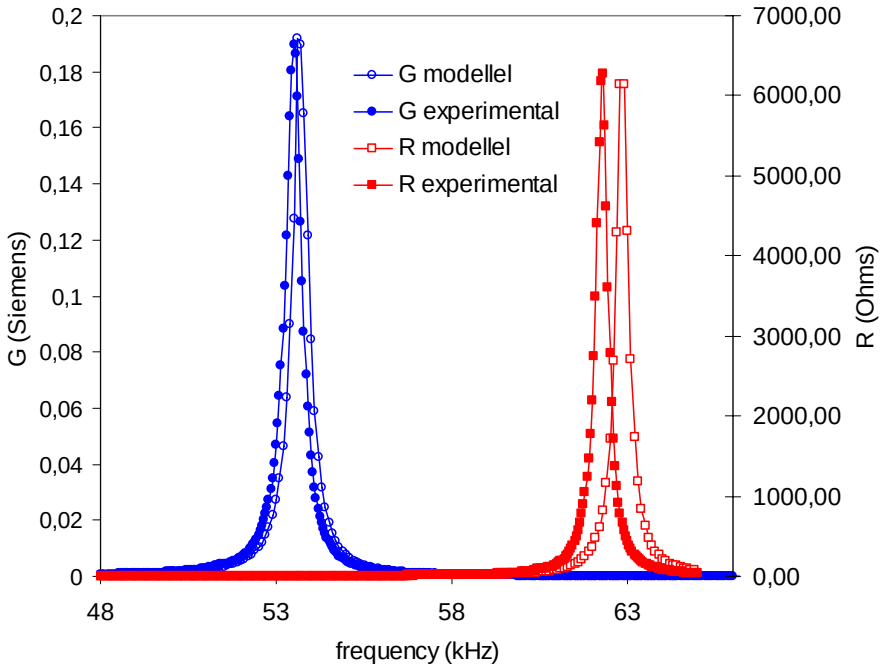

Figure 5. Experimental data and FEA modelled resistance, R, and conductance, G, using the improved matrix of parameters and for the fundamental radial resonance of a thin disk, thickness poled, of a Navy II type commercial PZT.

(a)

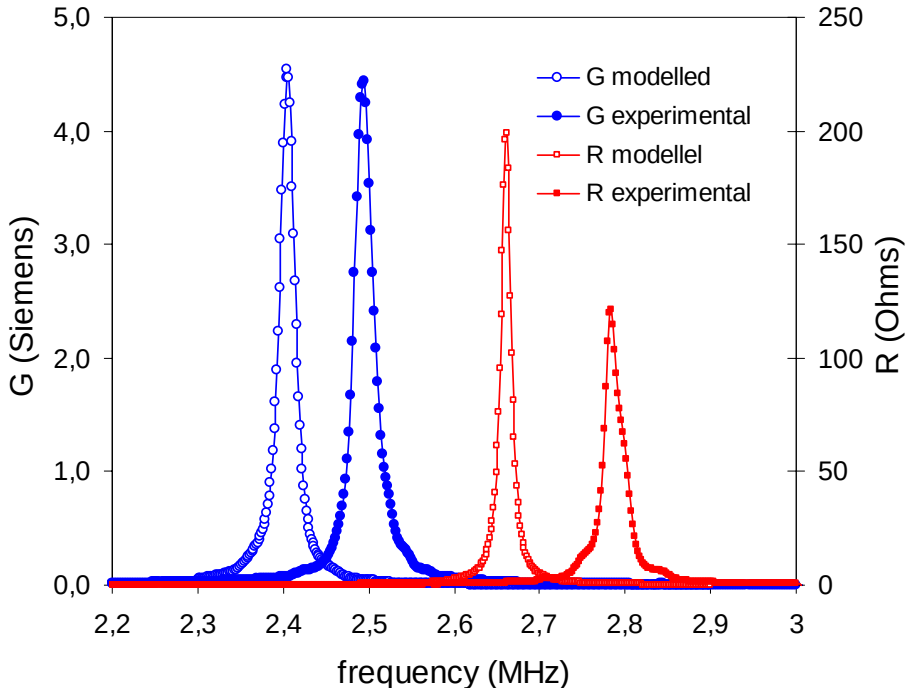

(b)

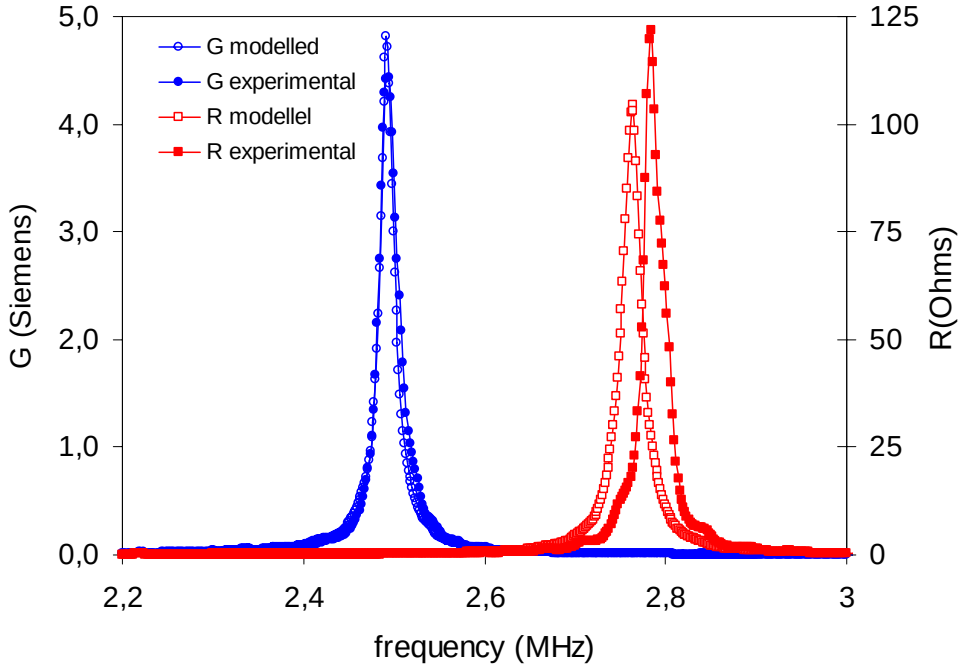

Figure 6. Experimental data and FEA generated resistance, R, and conductance, G, for the fundamental thickness resonance of a thin disk, thickness poled, of a Navy II type commercial PZT, (a) using the matrix of parameters including those shear parameters obtained from the IEEE Standard shear geometry (ref. 19) and (b) using the improved matrix of parameters of Figure 3.